applied sciences

MDPI

Article

Single-Crystalline $Si_{1-x}Ge_x$ (x = 0.5~1) Thin Films on Si (001) with Low Threading Dislocation Density Prepared by Low Temperature Molecular Beam Epitaxy

Yu Gu [1], Yunlei Zhao [2], Jiajia Ye [1], Yu Deng [1,3,*] and Hong Lu [1,*]

1 National Laboratory of Solid State Microstructures, College of Engineering and Applied Sciences and Collaborative Innovation Center of Advanced Microstructures, Nanjing University, Nanjing 210093, China; njuguyu@foxmail.com (Y.G.); yeyu93918@163.com (J.Y.)
2 School of Physics, Nanjing University, Nanjing 210093, China; yunlei.zhao@hpstar.ac.cn
3 Center of Modern Analysis, Nanjing University, Nanjing 210093, China
* Correspondence: dengyu@nju.edu.cn (Y.D.); hlu@nju.edu.cn (H.L.)

Received: 2 April 2019; Accepted: 24 April 2019; Published: 28 April 2019



Abstract: Single-crystalline $Si_{1-x}Ge_x$ thin films on Si (100) with low threading dislocation density (TDD) are highly desired for semiconductor industrials. It is challenging to suppress the TDD since there is a large mismatch (4.2%) between Ge and Si—it typically needs 10^6–10^7/cm^2 TDD for strain relaxation, which could, however, cause device leakage under high voltage. Here, we grew $Si_{1-x}Ge_x$ (x = 0.5–1) films on Si (001) by low temperature molecular beam epitaxy (LT-MBE) at 200 °C, which is much lower than the typical temperature of 450–600 °C. Encouragingly, the $Si_{1-x}Ge_x$ thin films grown by LT-MBE have shown a dramatically reduced TDD down to the 10^3–10^4/cm^2 level. Using transmission electron microscopy (TEM) with atomic resolution, we discovered a non-typical strain relaxation mechanism for epitaxial films grown by LT-MBE. There are multiple-layered structures being introduced along out-of-plane-direction during film growth, effectively relaxing the large strain through local shearing and subsequently leading to an order of magnitude lower TDD. We presented a model for the non-typical strain relaxation mechanism for $Si_{1-x}Ge_x$ films grown on Si (001) by LT-MBE.

Keywords: molecular beam epitaxy; thin film growth; $Si_{1-x}Ge_x$ films on Si (001); TEM characterizations; low threading dislocation density; strain relaxation mechanism

1. Introduction

Single-crystalline $Si_{1-x}Ge_x$ alloy films have been an important material system due to their tunable bandgaps, strains, and lattices, and they can be tuned to match III-V semiconductors [1,2]. Recently, they have become a more attractive topic for several reasons, such as to integrate GeSn on Si to produce direct bandgap Si photonic devices and to produce high-frequency microwave devices on Si [3–7]. Unfortunately, the large lattice mismatches (2.5–4.2%) between $Si_{1-x}Ge_x$ (x = 0.5–1) and Si (001) tend to relax through either serious "island growth" [8–10] or high TDD for the $Si_{1-x}Ge_x$ films grown on Si (001). It is known that all widely used Si-based devices, e.g., heterojunction bipolar transistor can suffer from the high TDD, as high-density dislocations penetrate the films and cause current leakage under high voltage [11–13]. Typically, the TDD in $Si_{1-x}Ge_x$ (x = 0.5–1) films grown on Si (001) can be controlled to the level of 10^6–10^7/cm^2 [14]. To effectively limit the TDD, as well as the "island growth" in $Si_{1-x}Ge_x$ films, many efforts were performed during the past decades [15–17]. For example, template-assisted selective epitaxy and selective-area epitaxy of nanostructures are good ways to help

acquire low TDD for technology developing on lasers, transistors, and photovoltaics, etc. [18–23] Among them, the LT-MBE (a few hundred degrees lower than the typical values [8]) was reported to be helpful for growing single-crystalline thin films with a high mismatch between substrate and the film [24,25]. It is believed that a thermal activation barrier is needed for the dislocation and planar defect nucleation [26,27], so a lower temperature can prevent the formation of dislocations. On the other hand, it is no good to grow $Si1_{-x}Ge_x$ films on Si (001) at an ultralow temperature [28–30], as it can eventually cause amorphous phases [31,32]. Therefore, in this study, we try to find a "proper" low temperature for the series of $Si1_{-x}Ge_x$·thin films on Si (001) grown by LT-MBE, including an appropriate treatment on the substrate, to prepare single-crystalline films with desired low TDD. TEM with atomic resolution has been used to characterize these films, and the film strain relaxation mechanism has been proposed.

2. Materials and Methods

Four $Si_{1-x}Ge_x$ (x = 0.5, 0.67, 0.8 and 1) films with equal thickness were grown on Si (001) in an Octoplus 300 MBE system, and a 6-kV e-beam evaporator for Si and an effusion cell for Ge are equipped. Thermal desorption procedure was used to remove the oxides on the Si (001) substrate, then a 30–50 nm Si buffer was grown at 700 °C and $Si_{1-x}Ge_x$ (x = 0.5, 0.67, 0.8 and 1) films were grown at 200 °C. Different Ge contents were controlled by varying the flux ratio of Si and Ge. X-ray diffraction (XRD) was used to characterize the crystal quality and noncontact mode atomic force microscope (AFM) was used to characterize the morphology. TDD was determined by measuring the etch pit density (EPD). The sample was etched for 30 s in Secco etchant [33]. Transmission electron microscopy (TEM) cross-sectional samples were initially hand-polished down to 10–20 μm. Ar+ ion milling with low energy and angle was the following step in order to obtain a thin region for sufficient TEM characterizations. FEI Tecnai F20 transmission electron microscope at acceleration voltage of 200 kV was used to obtain cross-sectional high resolution TEM (HRTEM) images.

3. Results and Discussion

We have conducted a series of experiments to find out the "proper" growth temperature for different Ge contents. $Si1_{-x}Ge_x$ films (20 nm thick) with x equals to 0.67 and 0.74 at growth temperatures of 100 °C, 200 °C, 300 °C, and 500 °C, respectively, were studied by XRD (see Figure 1). We have found that the full width at half maximum (FWHM) decreases as temperature decreases and AFM study (not shown here) also shows that the surface becomes smoother as temperature decreases down to 200 °C. Furthermore, for both $Si_{0.33}Ge_{0.67}$, and $Si_{0.26}Ge_{0.74}$ films grown at 200 °C, the fringes in the XRD spectra evidently indicate the well-crystallized interface between $Si_{1-x}Ge_x$ film and Si buffer layer. The film quality of the samples grown at 100 °C is comparable to the ones grown at 200 °C. As the growth temperature goes lower than a certain point, crystallization cannot be guaranteed beyond a critical thickness. Based on our study and the discussions above, we finally selected 200 °C as the "proper" low temperature for all the following film growth.

Figure 2a shows typical XRD spectra scanned from $Si_{0.5}Ge_{0.5}$ and Ge films grown on Si (001). Peaks of $Si_{0.5}Ge_{0.5}$ (004), Ge (004), and substrate Si (004) can be recognized. Figure 2b shows the low-magnification TEM image of $Si_{0.5}Ge_{0.5}$ film grown on Si (001). The selected area electron diffraction pattern (SAED) of $Si_{0.5}Ge_{0.5}$ film grown on Si (001) with zone axis of [110] is also shown and the SAED indicated the good coherency of the epitaxial growth. Figure 2c,d are AFM images of 4 μm × 4 μm area of $Si_{0.5}Ge_{0.5}$ and Ge films. It can be seen that no island growth occurred, and the film surface roughness remained in a few nanometers. The chemical etchant for TDD estimation was Secco etchant (1 part 0.15 mol/L $K_2Cr_2O_3$: 2-part 48% HF by volume) and etching time was 30 s. By counting the number of etch pits, TDD can be obtained as $3.33 \times 10^3/cm^2$ and $1.67 \times 10^4/cm^2$. The optical microscope images of typical $Si_{1-x}Ge_x$ films after etching are shown in Figure 2e,f, respectively. We chose three areas and took optical images. Here, the typical error bar is about ±10%. The TDD shows an average value of

10^3–10^4/cm^2, which is very low compared to the former reported data which was on the average of 10^6–10^7/cm^2.

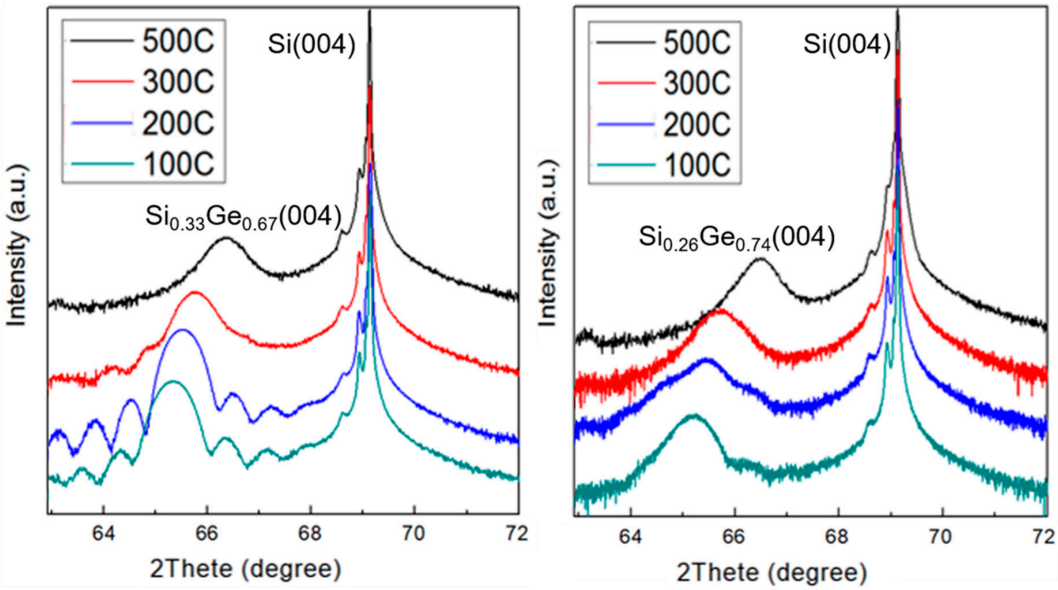


Figure 1. XRD spectra of series of $Si_{1-x}Ge_x$ thin films with x of 0.67 and 0.74, and growing temperatures of 100 °C, 200 °C, 300 °C, and 500 °C, respectively.

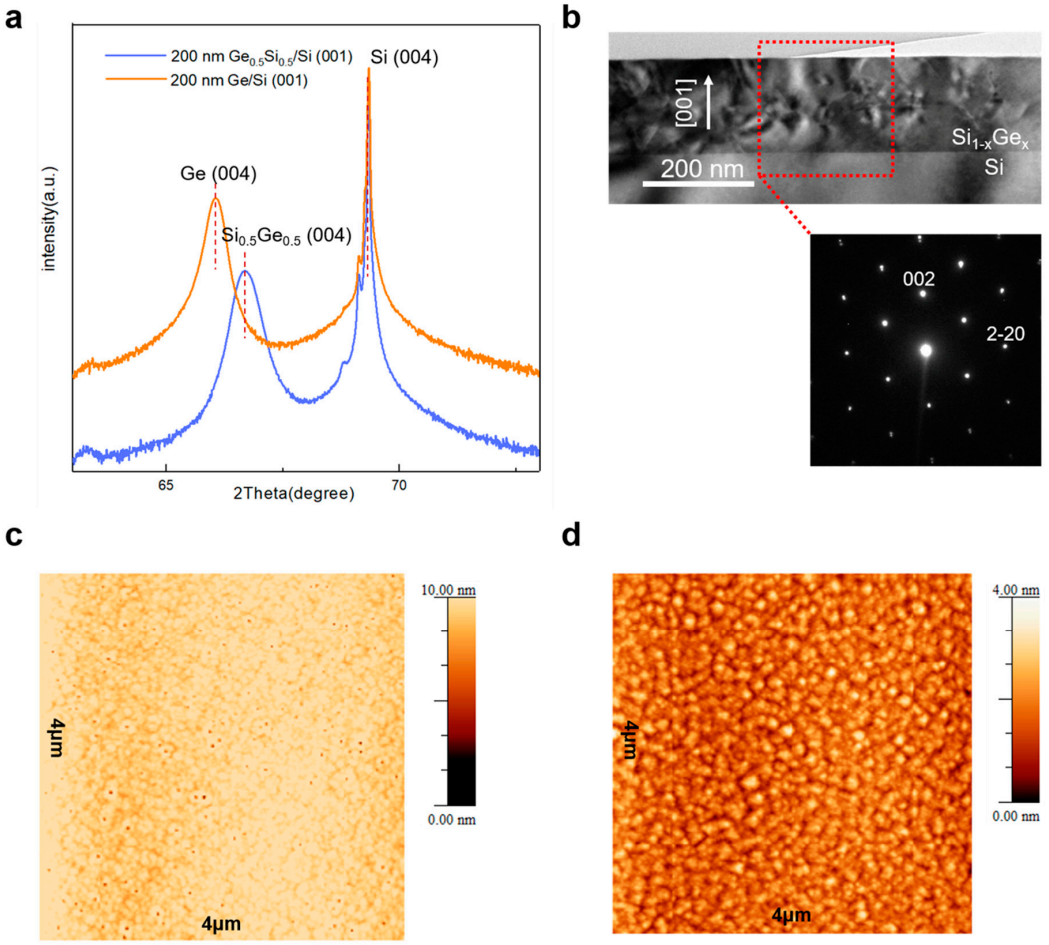


Figure 2. *Cont.*

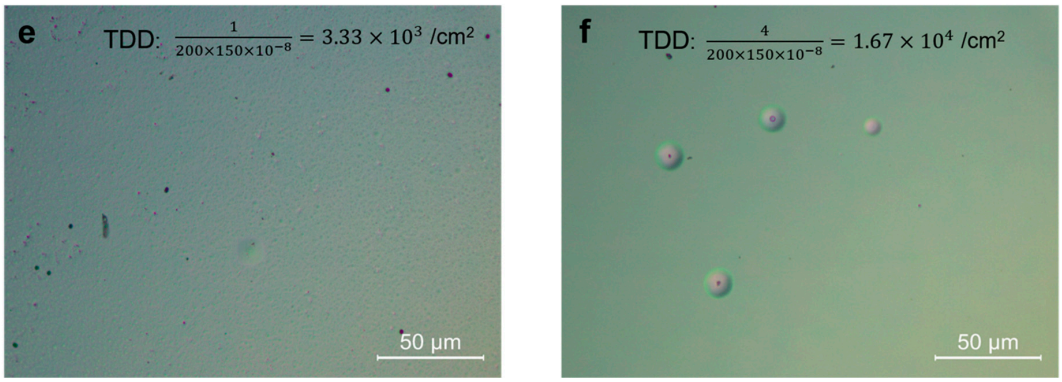


Figure 2. (**a**) XRD spectra of $Si_{0.5}Ge_{0.5}$ and Ge films grown on Si (001); (**b**) The SAED and low-magnification TEM image of the $Si_{0.5}Ge_{0.5}$ film grown on Si (001); (**c**,**d**) are AFM images of $Si_{0.5}Ge_{0.5}$ and Ge films, respectively; (**e**,**f**) shows the typical etch pits distribution of the $Si_{1-x}Ge_x$ thin films (x from 0.5 to 1), with TDD of 10^3–10^4/cm^2 level. The films were etched by Secco etchant. All films are 200 nm thick and grown at 200 °C.

As the dislocations nucleate at the free surface and glide to the interface, the atomic structure of dislocation at the heterointerface determines its electronic properties. In diamond structure, edge dislocations have higher core energy, thus strain relaxation prefers to occur by introducing 60°-mixed dislocations which lie on {111} gliding planes instead of edge dislocations. The misfit segments run in the <110> direction and the threading arms run up to the surface [24,34,35]. As Figure 3a shows, some 60° dislocations gliding towards the interface can be seen. For $Si_{1-x}Ge_x$ films grown on Si (001) by MBE under typical strain relaxation mechanism, as Ge content increases, lattice mismatch increases and more misfit dislocations at the interface and threading dislocations in the epilayer form. Figure 3a shows a HRTEM image of interface with dislocations and Figure 3b highlights the dislocation core. However, in this study, with the use of LT-MBE to grow $Si_{1-x}Ge_x$ films on Si (001), instead of seeing a great number of dislocations in the film due to large mismatch strain, an area containing multiple-layered structures and few dislocations were observed, as shown in Figure 3c. Figure 3d is the interface of Ge film and Si buffer layer containing multiple-layered structures and few dislocations. Very small local shearing (with around only 1° level orientation difference) at the interfaces of the multiple-layered structures can be clearly seen. However, the SAED shows that the film is still perfectly single-crystalline. Strain can be relaxed mainly through this kind of local shearing instead of forming a great number of dislocations. Thus, we found that area without multiple-layered structures relaxed strain through typical strain relaxation mechanism shows many dislocations, while area with multiple-layered structures shows few dislocations and it may be under a non-typical strain relaxation mechanism.

To understand the non-typical strain relaxation mechanism for $Si_{1-x}Ge_x$ films grown by LT-MBE, we studied the intermediate products of a pure Ge film with multiple-layered structures. Figure 4 shows the HRTEM images of multiple-layered structures imaging along zone axis of [110]. We found that there were partial "island growth," which left the hollow structures as shown in Figure 4I,II. Interestingly, the "partial islands" here are of approximately the same crystal orientation and finally merge into a single-crystalline structure during film growing (see Figure 4III). Therefore, this growth process by short "partial islands" and their merging lead to the multiple-layered structure in the film. Although being well-limited, here the "island growth" still causes small local orientation variations [14–16], leading to the local shearing at the interfaces of the multiple-layered structures. And the local shearing effectively relaxes the strain, subsequently suppresses the dislocation density. Based on above discussions, we know that the non-typical strain relaxation mechanism is actually related to a partial "island growth," which is strongly limited here (without any long pillar structures) and coexists with the typical strain relaxation mechanism.

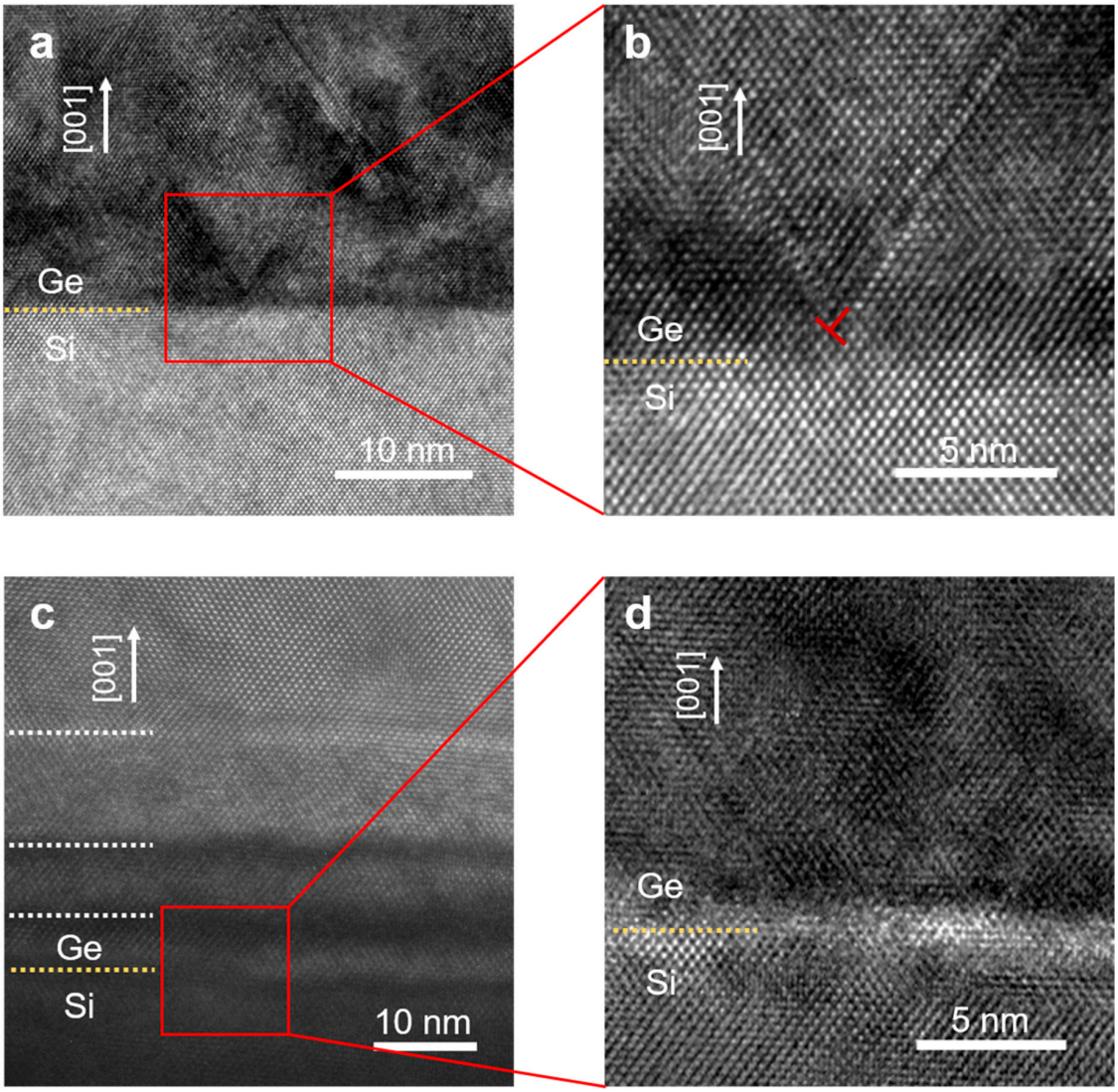


Figure 3. (**a**) Cross-sectional HRTEM image ([110]-zone) on an interface where strain is relaxed by dislocations; (**b**) zoom-in view of the red square marked in (**a**); (**c**) Cross-sectional HRTEM image ([110]-zone) an interface where strain is relaxed by the multiple-layered structures; (**d**) zoom-in view of the red square marked in (**c**). Yellow dotted lines highlight the interface of film and substrate. White dotted lines highlight the multiple-layered structures.

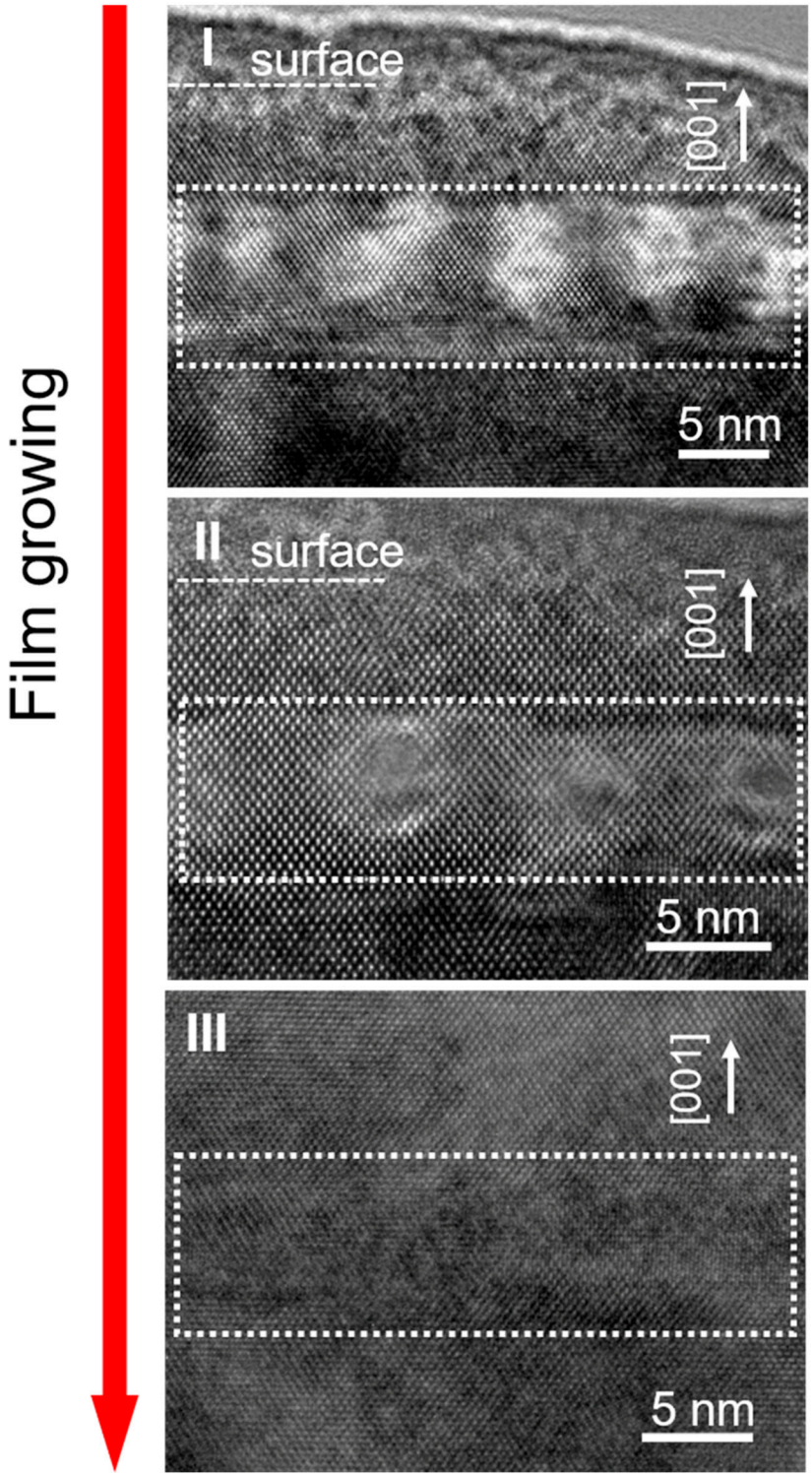


Figure 4. [110]-zone cross-sectional HRTEM images of the pure Ge film intermediate products, which actually show the process of non-typical strain relaxation for $Si_{1-x}Ge_x$ films grown by LT-MBE.

Figure 5 shows the schematic 2D model of the $Si_{1-x}Ge_x$ thin films grown on Si (001) relaxing strain through typical strain relaxation mechanism in an MBE grown heterostructure (circled in black on the left) together with the non-typical strain relaxation mechanism in an LT-MBE grown heterostructure (circled in black on the right). Red lines indicate the dislocations in the $Si_{1-x}Ge_x$ film. Blue lines indicate the local shearing at interfaces of multiple-layered structures. And the formation of multiple-layered

structures refers to the formation of short islands along [-110] direction and then the short islands will afterwards crystallize into a single-crystalline structure. The light grey cubes near the $Si_{1-x}Ge_x$ film surface indicate the short islands. Here, the low TDD of $Si_{1-x}Ge_x$ film may be attributed to such multiple-layered structures which can relax strain through local shearing [36–41]. As known, a typical growth temperature (e.g., 600 °C) for MBE growth, in general, means a sufficient surface diffusion for the adatoms and at the same time provides an annealing effect to remove the local shearing (i.e., inhomogeneous local strains). Practically, a high-temperature growth can always lead to a much more homogeneous thin film growth. Unfortunately, in this study, considering the large lattice mismatch (~4%) and thermal mismatch between Si and Ge, high-density dislocations becomes unavoidable in a "homogeneous" film, because other possible mechanisms for strain relaxation have been subsequently suppressed at higher temperatures. Another important factor in epitaxial growth is the surface preparation of the substrate. We found that as long as the surface is treated to be atomically smooth, there is still sufficient surface diffusion at lower temperatures even though the surface energy is reduced. Therefore, 200 °C seems to be a much lower temperature than a typical growth temperature in MBE, it can still provide enough surface energy for surface diffusion. Interestingly, we have found that the "relatively inhomogeneous" film grown at such a low temperature becomes a promising candidate, which can reach a point, where both poor crystallization and high-density dislocations are limited at the same time. We believe that the "non-typical strain relaxation mechanism" is as well useful for other thin film systems with a large mismatch between film and substrate.

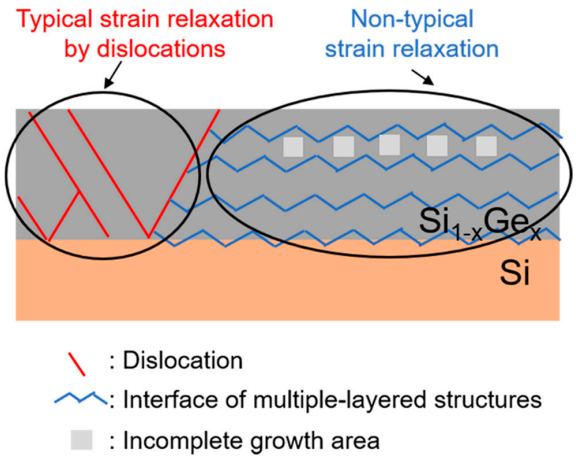


Figure 5. A schematic 2D model of the $Si_{1-x}Ge_x$ film relaxing strain by typical strain relaxation mechanism (circled on the left) together with the non-typical strain relaxation mechanism (circled on the right).

4. Conclusions

A series of $Si_{1-x}Ge_x$ thin films were grown on Si (001) by LT-MBE, displaying both smooth surface and good crystalline quality. TDDs of the $Si_{1-x}Ge_x$ films were measured to be as low as 10^3–10^4/cm^2, which is attributed to a non-typical strain relaxation mainly through local shearing instead of forming dislocations. Multiple-layered structures have been found in the out-of-plane direction of the $Si_{1-x}Ge_x$ films as a result of the local shearing. During LT-MBE, the non-typical strain relaxation mechanism has been discussed.

Author Contributions: Y.G. and H.L. conceived the study, Y.G., Y.Z., J.Y. and Y.D. performed the experiments, Y.G., Y.D. and H.L. interpreted and discussed the experiment results, and prepared the first draft of the manuscript, which was reviewed and edited by all authors.

Funding: This research was funded by the National Key R&D Program of China (2018YFA0306200, 2017YFA0303702), the National Nature Science Foundation of China (Grant No. 51732006, No. 11890702 and No. 11474158), the Natural Science Foundation of Jiangsu Province, China (Nos. BK20151382) and the Thousand Talents Program

Acknowledgments: Yu Gu would like to thank Yanbin Chen for TEM characterization and discussion. And Yu Deng like to thank Jiangsu Donghai Silicon Industry Science and Technology Innovation Center.

Conflicts of Interest: The authors declare no conflicts of interest.

References

1. Bakkers, E.P.; van Dam, J.A.; De Franceschi, S.; Kouwenhoven, L.P.; Kaiser, M.; Verheijen, M.; Wondergem, H.; van der Sluis, P. Epitaxial growth of InP nanowires on germanium. *Nat. Mater.* **2004**, *3*, 769–773. [CrossRef]
2. Liu, H.; Wang, T.; Jiang, Q.; Hogg, R.; Tutu, F.; Pozzi, F.; Seeds, A. Long-wavelength InAs/GaAs quantum-dot laser diode monolithically grown on Ge substrate. *Nat. Photonics* **2011**, *5*, 416–419. [CrossRef]
3. Lu Low, K.; Yang, Y.; Han, G.; Fan, W.; Yeo, Y.-C. Electronic band structure and effective mass parameters of Ge1-xSnx alloys. *J. Appl. Phys.* **2012**, *112*, 103715. [CrossRef]
4. Gupta, S.; Magyari-Köpe, B.; Nishi, Y.; Saraswat, K.C. Achieving direct band gap in germanium through integration of Sn alloying and external strain. *J. Appl. Phys.* **2013**, *113*, 073707. [CrossRef]
5. Wirths, S.; Geiger, R.; von den Driesch, N.; Mussler, G.; Stoica, T.; Mantl, S.; Ikonic, Z.; Luysberg, M.; Chiussi, S.; Hartmann, J.M.; et al. Lasing in direct-bandgap GeSn alloy grown on Si. *Nat. Photonics* **2015**, *9*, 88–92. [CrossRef]
6. Bhargava, N.; Coppinger, M.; Prakash Gupta, J.; Wielunski, L.; Kolodzey, J. Lattice constant and substitutional composition of GeSn alloys grown by molecular beam epitaxy. *Appl. Phys. Lett.* **2013**, *103*, 041908. [CrossRef]
7. Oehme, M.; Buca, D.; Kostecki, K.; Wirths, S.; Holländer, B.; Kasper, E.; Schulze, J. Epitaxial growth of highly compressively strained GeSn alloys up to 12.5% Sn. *J. Cryst. Growth* **2013**, *384*, 71–76. [CrossRef]
8. Brunner, K. Si/Ge nanostructures. *Rep. Prog. Phys.* **2001**, *65*, 27–72. [CrossRef]
9. Gao, H. Surface roughening of heteroepitaxial thin films. *Annu. Rev. Mater. Sci.* **1999**, *29*, 173–209. [CrossRef]
10. Ye, H.; Yu, J. Germanium epitaxy on silicon. *Sci. Technol. Adv. Mater.* **2014**, *15*, 024601. [CrossRef] [PubMed]
11. Tatsumi, T.; Hirayama, H.; Aizaki, N. Si/Ge0.3Si0.7/Si heterojunction bipolar transistor made with Si molecular beam epitaxy. *Appl. Phys. Lett.* **1988**, *52*, 895–897. [CrossRef]
12. Liu, Z. The Key Technologies in Silicon Based Microwave and RF MEMS Device Fabrication. In Proceedings of the 2004 4th International Conference on Microwave and Millimeter Wave Technology, Nanjing, China, 18–21 August 2004.
13. Giovane, L.M.; Luan, H.-C.; Agarwal, A.M.; Kimerling, L.C. Correlation between leakage current density and threading dislocation density in SiGe p-i-n diodes grown on relaxed graded buffer layers. *Appl. Phys. Lett.* **2001**, *78*, 541–543. [CrossRef]
14. Liu, Z.; Hao, X.; Huang, J.; Ho-Baillie, A.; Green, M.A. Reduction of Threading Dislocation Density in Sputtered Ge/Si(100) Epitaxial Films by Continuous-Wave Diode Laser-Induced Recrystallization. *ACS Appl. Energy Mater.* **2018**, *1*, 1893–1897. [CrossRef]
15. Choi, D.; Ge, Y.; Harris, J.S.; Cagnon, J.; Stemmer, S. Low surface roughness and threading dislocation density Ge growth on Si (001). *J. Cryst. Growth* **2008**, *310*, 4273–4279. [CrossRef]
16. Chen, D.; Xue, Z.; Wei, X.; Wang, G.; Ye, L.; Zhang, M.; Wang, D.; Liu, S. Ultralow temperature ramping rate of LT to HT for the growth of high quality Ge epilayer on Si (100) by RPCVD. *Appl. Surf. Sci.* **2014**, *299*, 1–5. [CrossRef]
17. Tan, Y.H.; Tan, C.S. Growth and characterization of germanium epitaxial film on silicon (001) using reduced pressure chemical vapor deposition. *Thin Solid Films* **2012**, *520*, 2711–2716. [CrossRef]
18. Convertino, C.; Zota, C.; Schmid, H.; Caimi, D.; Sousa, M.; Moselund, K.; Czornomaz, L. InGaAs FinFETs Directly Integrated on Silicon by Selective Growth in Oxide Cavities. *Materials* **2018**, *12*, 87. [CrossRef]
19. Borg, M.; Schmid, H.; Moselund, K.E.; Signorello, G.; Gignac, L.; Bruley, J.; Breslin, C.; Das Kanungo, P.; Werner, P.; Riel, H. Vertical III-V nanowire device integration on Si(100). *Nano Lett.* **2014**, *14*, 1914–1920. [CrossRef]
20. Ren, D.; Meng, X.; Rong, Z.; Cao, M.; Farrell, A.C.; Somasundaram, S.; Azizur-Rahman, K.M.; Williams, B.S.; Huffaker, D.L. Uncooled Photodetector at Short-Wavelength Infrared Using InAs Nanowire Photoabsorbers on InP with p-n Heterojunctions. *Nano Lett.* **2018**, *18*, 7901–7908. [CrossRef] [PubMed]
21. Ren, D.; Farrell, A.C.; Williams, B.S.; Huffaker, D.L. Seeding layer assisted selective-area growth of As-rich InAsP nanowires on InP substrates. *Nanoscale* **2017**, *9*, 8220–8228. [CrossRef] [PubMed]

22. Kim, H.; Ren, D.; Farrell, A.C.; Huffaker, D.L. Catalyst-free selective-area epitaxy of GaAs nanowires by metal-organic chemical vapor deposition using triethylgallium. *Nanotecnology* **2018**, *29*, 085601. [CrossRef]
23. Li, Q.; Ng, K.W.; Tang, C.W.; Lau, K.M.; Hill, R. Defect reduction in epitaxial InP on nanostructured Si (001) substrates with position-controlled seed arrays. *J. Cryst. Growth* **2014**, *405*, 81–86. [CrossRef]
24. Bean, J.C.; Sheng, T.T.; Feldman, L.C.; Fiory, A.T.; Lynch, R.T. Pseudomorphic growth of GexSi1−xon silicon by molecular beam epitaxy. *Appl. Phys. Lett.* **1984**, *44*, 102–104. [CrossRef]
25. Halbwax, M.; Bouchier, D.; Yam, V.; Débarre, D.; Nguyen, L.H.; Zheng, Y.; Rosner, P.; Benamara, M.; Strunk, H.P.; Clerc, C. Kinetics of Ge growth at low temperature on Si(001) by ultrahigh vacuum chemical vapor deposition. *J. Appl. Phys.* **2005**, *97*, 064907. [CrossRef]
26. Mooney, P.M. Strain relaxation and dislocations in SiGe/Si structures. *Mater. Sci. Eng.* **1996**, *17*, 105–146. [CrossRef]
27. LeGoues, F.K.; Mooney, P.M.; Tersoff, J. Measurement of the activation barrier to nucleation of dislocations in thin films. *Phys. Rev. Lett.* **1993**, *71*, 396–399. [CrossRef]
28. Faleev, N.; Sustersic, N.; Bhargava, N.; Kolodzey, J.; Magonov, S.; Smith, D.J.; Honsberg, C. Structural investigations of SiGe epitaxial layers grown by molecular beam epitaxy on Si(001) and Ge(001) substrates: II—Transmission electron microscopy and atomic force microscopy. *J. Cryst. Growth* **2013**, *365*, 35–43. [CrossRef]
29. Chen, X.; Zuo, D.; Kim, S.; Mabon, J.; Sardela, M.; Wen, J.; Zuo, J.-M. Large Area and Depth-Profiling Dislocation Imaging and Strain Analysis in Si/SiGe/Si Heterostructures. *Microsc. Microanal.* **2014**, *20*, 1521–1527. [CrossRef]
30. Bolkhovityanov, Y.B.; Deryabin, A.S.; Gutakovskii, A.K.; Revenko, M.A.; Sokolov, L.V. Strain relaxation of GeSi/Si(001) heterostructures grown by low-temperature molecular-beam epitaxy. *J. Appl. Phys.* **2004**, *96*, 7665–7674. [CrossRef]
31. Eaglesham, D.J.; Cerullo, M. Low-temperature growth of Ge on Si(100). *Appl. Phys. Lett.* **1991**, *58*, 2276–2278. [CrossRef]
32. Bauer, M.; Lyutovich, K.; Oehme, M.; Kasper, E.; Herzog, H.J.; Ernst, F. Relaxed SiGe buffers with thicknesses below 0.1 mm. *Thin Solid Films* **2000**, *369*, 152–156. [CrossRef]
33. d'Aragona, F.S. Dislocation Etch for (100) Planes in Silicon. *J. Electrochem. Soc.* **1972**, *119*, 948–951.
34. Narayan, J. Recent progress in thin film epitaxy across the misfit scale (2011 Acta Gold Medal Paper). *Acta Mater.* **2013**, *61*, 2703–2724. [CrossRef]
35. Marée, P.M.J.; Barbour, J.C.; van der Veen, J.F.; Kavanagh, K.L.; Bulle-Lieuwma, C.W.T.; Viegers, M.P.A. Generation of misfit dislocations in semiconductors. *J. Appl. Phys.* **1987**, *62*, 4413–4420. [CrossRef]
36. Matt Law, J.G.; Yang, P. Semiconductor nanowires and nanotubes. *Annu. Rev. Mater. Res.* **2004**, *34*, 83–122.
37. Wu, Y.; Fan, R.; Yang, P. Block-by-Block Growth of Single-Crystalline Si/SiGe Superlattice Nanowires. *Nano Lett.* **2002**, *2*, 283–286. [CrossRef]
38. Wu, Y.; Yang, P. Direct Observation of Vapor-Liquid-Solid Nanowire Growth. *J. Am. Chem. Soc.* **2001**, *123*, 3165–3166. [CrossRef]
39. Chen, K.; Kapadia, R.; Harker, A.; Desai, S.; Seuk Kang, J.; Chuang, S.; Tosun, M.; Sutter-Fella, C.M.; Tsang, M.; Zeng, Y.; et al. Direct growth of single-crystalline III-V semiconductors on amorphous substrates. *Nat. Commun.* **2016**, *7*, 10502. [CrossRef]
40. Zheng, M.; Horowitz, K.; Woodhouse, M.; Battaglia, C.; Kapadia, R.; Javey, A. III-Vs at scale: A PV manufacturing cost analysis of the thin film vapor-liquid-solid growth mode. *Prog. Photovolt. Res. Appl.* **2016**, *24*, 871–878. [CrossRef]
41. Hettick, M.; Zheng, M.; Lin, Y.; Sutter-Fella, C.M.; Ager, J.W.; Javey, A. Nonepitaxial Thin-Film InP for Scalable and Efficient Photocathodes. *J. Phys. Chem. Lett.* **2015**, *6*, 2177–2182. [CrossRef]



© 2019 by the authors. Licensee MDPI, Basel, Switzerland. This article is an open access article distributed under the terms and conditions of the Creative Commons Attribution (CC BY) license (http://creativecommons.org/licenses/by/4.0/).